

# Faujasite Catalysts Promoted with Gallium Oxide: A Physicochemical Study

B. Sulikowski,<sup>\*,†</sup> Z. Olejniczak,<sup>‡</sup> and V. Cortés Corberán<sup>§</sup>

*Institute of Catalysis and Surface Chemistry, Polish Academy of Sciences, Niezapominajek 1, 30-239 Kraków, Poland, Institute of Nuclear Physics, Radzikowskiego 152, 31-342 Kraków, Poland, and Instituto de Catálisis y Petroleoquímica, C.S.I.C., Campus U.A.M.-Cantoblanco, 28049 Madrid, Spain*

Received: February 13, 1996<sup>®</sup>

This paper examines the properties of a defected zeolite matrix with the faujasite structure, promoted with gallium oxide. The fate of  $\beta$ -Ga<sub>2</sub>O<sub>3</sub> loaded onto ultrastable faujasite is followed by XRD, FT IR, and laser Raman spectroscopies, and also by solid-state multinuclear NMR. Gallium(III) oxide is reduced after the contact with the zeolite, which is demonstrated by XRD, FT IR, and Raman measurements. Reduced gallium oxide is transferred to the channel system of the faujasite matrix, and some of the gallium ions (up to 6/unit cell) are occupying the zeolite tetrahedral sites, as evidenced by <sup>29</sup>Si and <sup>71</sup>Ga MAS NMR and IR studies. The Si/Al ratio of the matrix changes during this process. Gallium sites of the type Si–O(H)–Ga can be discerned in IR spectra as a 3600–3603 cm<sup>-1</sup> band of the OH group. Such hydroxyl groups, not present in the pure faujasitic matrix, interact with ammonia. The gallium-promoted catalysts were tested in the oxidative dehydrogenation of propane. It will be shown that the already few gallium ions introduced into the faujasitic matrix significantly increase the selectivity of propane conversion to propene.

## Introduction

Gallium-containing zeolites constitute a very interesting class of solids from a catalytic standpoint. The gallium analogue of ZSM-5 (MFI) is used for transformation of C<sub>3</sub>–C<sub>5</sub> alkanes into aromatic hydrocarbons.<sup>1</sup> For example, conversion of propane in the Cyclar process yields 63.1 wt % benzene, toluene, xylene (BTX), hydrogen (5.9 wt %), and a fuel gas byproduct containing mainly methane and ethane.<sup>2</sup> The Ga<sup>3+</sup> ions in zeolites can occupy tetrahedral framework sites (T) and non-framework (NF, or extraframework) cationic positions. Gallium has been successfully introduced into numerous zeolite frameworks by direct hydrothermal synthesis.<sup>3</sup> Gallium can also be inserted into solids *via* postsynthesis treatment of silica polymorphs or high-silica zeolites by using sodium gallate. In this way galliation of Silicalite-II (MEL)<sup>4</sup> and recently of zeolite Beta (BEA)<sup>5</sup> has been accomplished. The isomorphous substitution of gallium into aluminosilicate zeolites results in enhanced selectivity toward aromatic hydrocarbons. It is interesting to note that not only deliberately synthesized [Si,Ga]-ZSM-5 molecular sieves containing framework gallium were the active catalysts. Dehydrogenation properties were also induced by mechanical mixing of the standard ZSM-5 zeolite and Ga<sub>2</sub>O<sub>3</sub>.<sup>6</sup> Such mixtures after a proper pretreatment were the active catalysts for dehydrogenation of lower alkanes.<sup>7</sup> Most of the research has been focused on the Ga<sub>2</sub>O<sub>3</sub>-MFI<sup>1,6–8</sup> and Ga<sub>2</sub>O<sub>3</sub>-MEL systems.<sup>4,9–10</sup> The status of gallium in MFI is a much discussed issue, because of considerations concerning the mechanism of low-alkane aromatization. On the other hand, there is a dearth of information on the interaction of Ga<sub>2</sub>O<sub>3</sub> with other zeolites. We wish to report on the physicochemical properties of catalysts based on a zeolite having a pore system wider than that of ZSM-5. For this purpose zeolite Y, a 12-membered ring aluminosilicate, has been chosen. The acid-extracted ultrastable form of zeolite Y was used due to its known

resistance to temperature. The conversion of propane in the presence of oxygen has been chosen as a test reaction. Gallium(III) oxide, a pure zeolitic matrix, and the matrix loaded with different amounts of Ga<sub>2</sub>O<sub>3</sub> were investigated in this process.

## Experimental Section

**Catalyst Preparation.** The ultrastable sample was prepared by a procedure combining hydrothermal treatment of zeolite Na–Y,<sup>11,12</sup> followed by acid leaching.<sup>13–15</sup> Zeolite Na–Y, highly crystalline to X-rays, with Si/Al = 2.47 and Na/Al = 1.09 determined by atomic absorption (AA), was used as the parent material. The zeolite was twice ammonium exchanged by stirring with 10 wt % NH<sub>4</sub>Cl at 368 K for 1 h. The ammonium form (0.76 NH<sub>4</sub>, Na–Y, 25.81 wt % loss of ignition) was heated in a horizontal quartz reactor at 813 K for 4 h under self-steaming conditions. The ion exchange was then repeated, and the sample was calcined at 1093 K to yield the ultrastable form (US–Y) with Si/Al = 2.55 and Na/Al = 0.003 (bulk, determined by AA). This form was treated twice with 1 dm<sup>3</sup> of 0.1 and 0.2 M HCl per 100 g of the sample at 464 K for 1 h, washed with water, and dried. The acid-extracted ultrastable zeolite (US–Y-ex) had Si/Al = 8.91 (bulk) and Na/Al = 0.003 and was used as a matrix (M). The matrix was ground in an agate mortar with spectroscopically pure  $\beta$ -Ga<sub>2</sub>O<sub>3</sub> (Bi, Cr, Zn, Sn, Al, Co, and Fe: the content of each metal < 10<sup>-4</sup> wt %; In, Mg, Mn, Cu and Pb < 5 × 10<sup>-5</sup> wt %; BET<sub>Ar</sub> = 2.90 m<sup>2</sup>/g).  $\alpha$ -Ga<sub>2</sub>O<sub>3</sub> from Aldrich (containing ca. 5 wt %  $\beta$ -phase, BET<sub>Ar</sub> = 27.5 m<sup>2</sup>/g) was used in some experiments. The hybrid catalysts containing 4.8–44.4 wt %  $\beta$ -Ga<sub>2</sub>O<sub>3</sub> were calcined in air or reduced in hydrogen at 473–873 K prior to characterization. The samples for reduction were heated at a rate of 3 K/min in a nitrogen flow (30 cm<sup>3</sup>/min). The reduction with hydrogen (20 cm<sup>3</sup>/min) was performed for 2 h followed by cooling the samples to ambient temperature in a dry nitrogen flow. Mixed samples will be labeled hereafter for brevity as *x* Ga/M, where *x* denotes the initial amount of  $\beta$ -Ga<sub>2</sub>O<sub>3</sub> in the sample (wt %) and M represents the zeolitic matrix US–Y-ex.

**Characterization.** Powder XRD patterns of the fully hydrated samples were acquired on Seifert XRD 3000P and Dron-2 diffractometers using Ni-filtered Cu K $\alpha$  radiation.

\* Corresponding author. Telephone: (+48 12) 252841. FAX: (+48 12) 251923. E-mail: ncsuliko@cyf-kr.edu.pl.

<sup>†</sup> Polish Academy of Sciences.

<sup>‡</sup> Institute of Nuclear Physics.

<sup>§</sup> Instituto de Catálisis y Petroleoquímica C.S.I.C.

<sup>®</sup> Abstract published in *Advance ACS Abstracts*, May 15, 1996.

High-resolution solid-state magic-angle-spinning (MAS) NMR spectra were recorded at 6.3 T (53.713 and 70.456 MHz for  $^{29}\text{Si}$  and  $^{27}\text{Al}$ , respectively).  $^{29}\text{Si}$  MAS NMR spectra were acquired with  $\pi/2$  pulses and a repetition time of 10 s.  $^{27}\text{Al}$  MAS NMR spectra were obtained using very short (1  $\mu\text{s}$ ) pulses with 25 kHz  $B_1$  amplitude to ensure that they are quantitatively reliable.<sup>16,17</sup> The recycle delays were 0.5 s. Typically, 1000 and 4000 transients were accumulated for silicon and aluminum spectra. The rotors were spun in air at 4 kHz.  $^{71}\text{Ga}$  MAS NMR spectra were acquired on a Bruker ASX 500 spectrometer operating at 152.514 MHz. Samples were spun in air at 14 kHz, and 1  $\mu\text{s}$  radio frequency pulses were applied with 1 s recycle delay. Chemical shifts are quoted in ppm from external tetramethylsilane (TMS), aluminum nitrate, and  $(\text{NH}_4)\text{Ga}(\text{SO}_4)_2$  for silicon, aluminum, and gallium, respectively.

The IR spectra in the zeolite framework vibration region were obtained with a Nicolet 800 FT spectrometer (resolution 1  $\text{cm}^{-1}$ ) using the KBr technique. The same spectrometer was used for recording the spectra of self-supported disks and to monitor the interaction of ammonia with the hydroxyl groups. All the samples were evacuated at 600  $^\circ\text{C}$  and ca.  $10^{-7}$  Torr prior to measurement. Laser Raman FT spectra of the hydrated samples were collected with the Raman module of the Nicolet 800 spectrometer. A Nd:YAG laser was used as the excitation source ( $\lambda = 1046$  nm), and the beam power on the sample was adjusted as necessary (50–600 mW). The sample was placed in a Raman cell, and the scattered light was detected with a liquid-nitrogen-cooled germanium detector. The correction of background due to the Rayleigh scattering and the correction for white light was performed by use of Nicolet software.

Argon sorption at the temperature of liquid nitrogen was measured in a volumetric sorption unit of standard design. The samples were outgassed at 623 K before sorption studies.

**Catalytic Tests.** Catalyst particles (ca. 0.1 g, 0.25–0.42 mm) were loaded into a tubular down-flow quartz reactor. SiC chips were placed above the zeolite particles up to a total bed volume of 1  $\text{cm}^3$ . The catalyst was preheated in a flow of dry helium (100  $\text{cm}^3/\text{min}$ ) at 773 K for 1 h. The propane (99.9%)–oxygen (99.99%) mixture (2:1 molar ratio) diluted with helium was fed into the reactor to give a total flow of 100  $\text{cm}^3/\text{min}$  and  $W/F = 4$  g cat h/(g mol  $\text{C}_3$ ). The conversion of propane was studied at temperatures in the range 773–873 K under atmospheric pressure. Special precautions have been undertaken to suppress the homogeneous reaction of propane. Reactants and products were analyzed on-line with a Varian 3400 gas chromatograph equipped with a TCD detector. Two columns loaded with Porapak QS and molecular sieve were used for analysis.

## Results and Discussion

The hydrogen form of zeolite Y is unstable thermally;<sup>18</sup> therefore we prepared for our experiments the matrix with an increased silicon to aluminum framework ratio. This was done by use of a procedure described in the Experimental Section.

$^{29}\text{Si}$  MAS NMR spectra of parent zeolite Na-Y, the ultrastable matrix, and the matrix loaded with different amounts of  $\beta\text{-Ga}_2\text{O}_3$  and reduced by hydrogen are shown in Figures 1 and 2. The  $^{29}\text{Si}$  spectra in these figures consist of up to five signals, depending on composition. The signals correspond to five different possible environments of a silicon atom  $\text{Si}(n\text{Al})$ , where  $n$  ( $n \leq 4$ ) denotes the number of aluminum atoms connected, *via* oxygens, to a central silicon atom. The silicon to aluminum ratio of the zeolitic framework can be calculated directly from the  $^{29}\text{Si}$  MAS NMR spectrum using the formula<sup>19</sup>

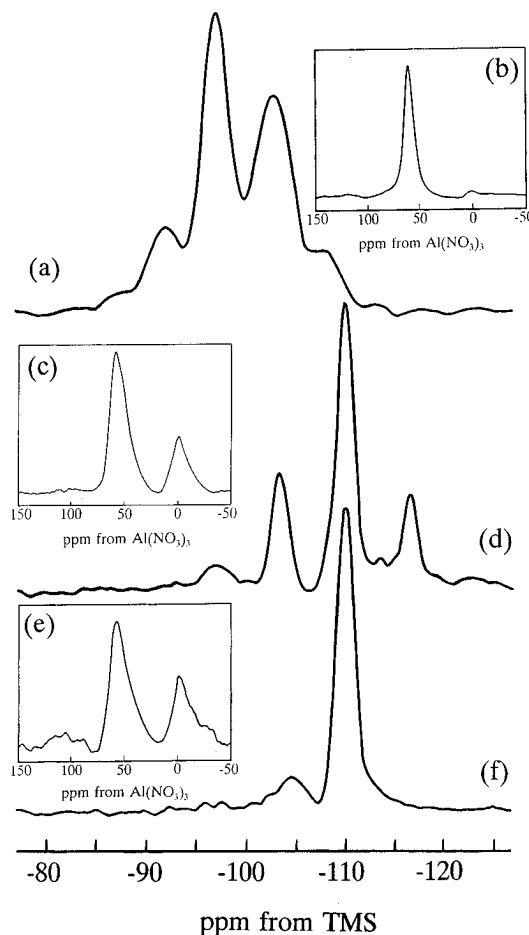


**Figure 1.**  $^{29}\text{Si}$  (a, d, f) and  $^{27}\text{Al}$  (b, c, e) solid-state MAS NMR spectra of Na-Y (a, b), US-Y-ex (M) (c, d), and 4.8 Ga/M (e, f). The 4.8 Ga/M sample was reduced with hydrogen prior to measurement (as in Figure 2).

$$(\text{Si}/\text{Al})_{\text{NMR}} = \frac{\sum_{n=0}^4 I_n}{I_4 + 0.75I_3 + 0.5I_2 + 0.25I_1}$$

where  $I_n$  denotes the intensity of the NMR signal corresponding to the  $\text{Si}(n\text{Al})$  grouping. The formula provides a reliable quantitative method for the determination of framework compositions of crystalline aluminosilicates (cf., for example, ref 20). The  $(\text{Si}/\text{Al})_{\text{NMR}}$  ratios of the framework, calculated from the above formula, are listed in Table 3.

The parent sample Na-Y had 55.6 Al in the framework, as evidenced by NMR spectra (Figure 1a,b). After hydrothermal treatment, 22.4 Al atoms have been expelled into extraframework positions to give sample US-Y with 33.2 aluminum ions in the framework (Table 1). The US-Y sample was additionally treated with HCl to remove nonframework aluminum and to extract more tetrahedral Al. Mineral acids can be used for extraction of aluminum from high-silica aluminosilicates (e.g., clinoptilolite,<sup>21</sup> and faujasite is also amenable to acid treatment.<sup>22</sup> Acid treatment of the US-Y sample, yielding the US-Y-ex matrix, did not affect its XRD crystallinity, as revealed by examination of the corresponding diffractograms. Also, the BET surface area of US-Y-ex (599  $\text{m}^2$ ) remained the same in comparison with the parent Na-Y material (Table 1). Thus, the procedure applied led neither to the amorphization of the solid nor to a decrease in its sorption capacity.

As seen from Table 1, most of the extraframework aluminum generated during hydrothermal treatment was indeed removed.

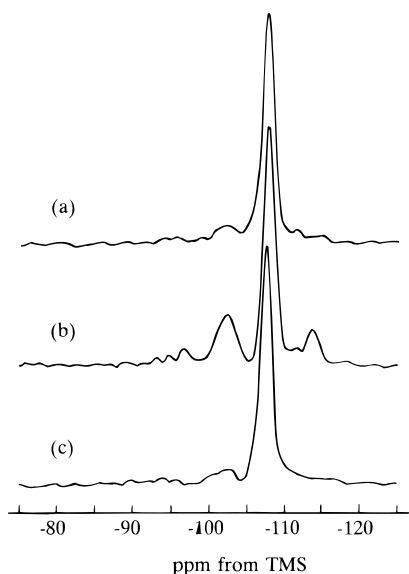


**Figure 2.**  $^{29}\text{Si}$  MAS NMR spectra of (a) 9.1 Ga/M, (b) 16.7 Ga/M, and (c) 28.6 Ga/M. All the samples were reduced with  $\text{H}_2$  at 600 °C for 2 h prior to measurement.

Moreover, some aluminum atoms were extracted from *tetrahedral* sites, thus creating vacancies in the aluminosilicate framework. Approximately 19  $\text{Al}_\text{F}$  atoms per unit cell were extracted from US-Y by HCl, and hence the same number of defects was introduced into the US-Y-ex matrix (note that M was not healed under hydrothermal conditions *prior* to loading with gallium oxide). It was supposed that such a defected matrix would easily react with or accommodate gallium oxide. The total silicon to aluminum ratio equals to 8.91 for US-Y-ex (M); this corresponds to 19.4 Al per unit cell. Aluminum in the sample is distributed between tetrahedral and octahedral positions. The number of aluminum atoms in the framework of zeolites X and Y affects their unit cell parameters as well as most of the mid-infrared frequencies, largely because Si–O bonds are shorter than Al–O bonds (1.60 Å and 1.75 Å). Empirical formulas were therefore derived that allow estimation of the number of Al atoms occupying framework sites in faujasite.<sup>23–25</sup> All the formulas, despite the method used for aluminum depletion,<sup>26</sup> give reasonable results.

The number of *framework* aluminum atoms in the matrix was calculated from the unit cell parameter contraction, the shift of the Si–O main asymmetric stretching band in IR, and deconvolution of  $^{29}\text{Si}$  MAS NMR (cf. Figure 1d). The sample contains 11.3 and 11.5  $\text{Al}_\text{F}$  according to IR,<sup>23,24</sup> 15.7 and 14.5 from XRD measurements,<sup>23,25</sup> 12.7 and 16.7 according to  $^{27}\text{Al}$  and  $^{29}\text{Si}$  MAS NMR spectra, respectively. The average number of aluminum occupying framework positions of the matrix, estimated from four independent methods, is therefore 14.0/uc (uc = unit cell).

As revealed by  $^{27}\text{Al}$  NMR, the matrix still contains a few atoms (5.4  $\text{Al}_\text{NF}$ ) of nonframework aluminum in the unit cell, which have not been extracted by HCl under the conditions specified. Distribution of the  $\text{Al}_\text{NF}$  species in zeolite Y depends on the temperature of hydrothermal treatment.<sup>27</sup> Treatment at 573 K gave samples with octahedrally coordinated aluminum entities located in the large cavities, while increasing the temperature to 773 K yielded the sample with  $\text{Al}_\text{NF}$  located in both the large cavities and sodalite cages. Our sample was calcined at higher temperature, so it is reasonable to assume that some or all of the nonframework aluminum is occupying hindered positions (sodalite cages and/or hexagonal prisms) and thus not amenable to extraction by mineral acid.

**TABLE 1: Characteristics of the Parent Material and Gallium-Loaded Zeolitic Catalysts**

sample	Si/Al <sup>a</sup>	lattice constant (Å) <sup>b</sup>	BET (argon) (m <sup>2</sup> /g)	Al <sub>F</sub> /uc (average)
Na–Y	2.47	24.690(2)	599	55.6
US–Y	2.55	24.51(1)		33.2
US–Y-ex (M)		24.373(5)	599	14.0
4.8 Ga/M	8.91	24.382(5)	432	8.3
9.1 Ga/M		24.406(4)	580	9.4
16.7 Ga/M		24.431(3)	472	11.1
28.6 Ga/M		24.50(2) <sup>c</sup>	403	8.0

<sup>a</sup> Bulk, by wet chemical analysis (AA). <sup>b</sup> Lattice parameters were calculated for the fully hydrated samples. <sup>c</sup> After reduction with hydrogen at 873 K for 2 h.

**TABLE 2: Number of Aluminum Atoms in the Reduced Catalysts, Occupying Framework (F) and Nonframework (NF) Sites, As Derived from  $^{27}\text{Al}$  MAS NMR Studies**

sample	calculated from $^{27}\text{Al}$ NMR			Al/uc not seen by NMR
	Al <sub>F</sub> /uc	Al <sub>NF</sub> /uc	(Al <sub>F</sub> + Al <sub>NF</sub> )/uc	
4.8 Ga/M	10.0	3.5	13.5	5.9
9.1 Ga/M	10.5	3.4	13.9	5.5
16.7 Ga/M	10.7	3.0	13.7	5.7
28.6 Ga/M	8.4	3.4	11.8	7.6

**TABLE 3: Number of Aluminum and Gallium Ions at Framework Sites in the Catalysts, As Calculated from NMR Studies**

sample	Al <sub>F</sub> /uc			Ga <sub>F</sub> /uc $^{29}\text{Si}$ NMR
	$^{27}\text{Al}$ NMR	$^{29}\text{Si}$ NMR	average	
Na–Y	55.6	55.6	55.6	
US–Y	nd	33.2	33.2	
US–Y-ex (M)	12.7	16.7	14.0 <sup>a</sup>	
4.8 Ga/M	10.0	6.6	8.3	3.6
9.1 Ga/M	10.5	8.3	9.4	2.2
16.7 Ga/M	10.7	11.5	11.1	5.9
28.6 Ga/M	8.4	7.5	8.0	3.6

<sup>a</sup> Mean value, calculated from  $^{27}\text{Al}$  and  $^{29}\text{Si}$  MAS NMR, IR, and XRD.

In the  $^{29}\text{Si}$  spectrum of the matrix an additional signal at  $-114.7$  ppm is clearly seen (Figure 1d), with an intensity of 17.5%. This line is assigned to nonordered Si(0Al) groupings of amorphous silica, which are formed during the matrix preparation. The silicon signals in this range have also been observed in zeolites dealuminated by  $\text{SiCl}_4$ .<sup>28,29</sup> After loading with gallium oxide and reduction with hydrogen this signal vanishes (Figures 1f and 2a,c). Silicon and gallium species are therefore competing for healing the matrix defects; and as will be discussed below, it is mostly silicon which is inserted into tetrahedral zeolitic sites. In the gallium-containing samples dealumination is proceeding further. Approximately 5–7  $\text{Al}_\text{F}$  atoms are expelled into nonframework positions, and vacancies formed are healed with silicon coming from amorphous-like silicon species giving rise to a signal at  $-114.7$  ppm. Close inspection of the  $x$  Ga/M  $^{29}\text{Si}$  spectra (Figures 1 and 2) revealed that, besides lines of Si(1Al) and Si(2Al) groups at  $-102$  and  $-96$  ppm, weak signals at  $-100$  and  $-94$  ppm were present. The signals were assigned to Si(1Ga) and Si(2Ga) groupings, respectively, taking into account published data on the as-prepared gallosilicates with the faujasite structure.<sup>30</sup> Gaussian deconvolution of the silicon spectra gave Si/Al and Si/Ga ratios in the samples. Distribution of aluminum between framework and nonframework positions was also calculated independently from  $^{27}\text{Al}$  spectral data. The data thus obtained are summarized in Tables 1–3. As seen, there is a fairly good agreement between the quantitative estimation of silicon, aluminum, and

gallium ions in the framework of catalysts, carried out by different approaches.

The characterization of the starting materials and the gallium-containing samples is given in Table 1. The crystallinity of all of the gallium-loaded samples was largely retained upon thermal treatment in air and hydrogen. Thermal treatment of the sample up to 673 K did not affect the crystallinity of the matrix. For the 28.6 Ga/M sample reduced at 873 K the decreased XRD crystallinity of the matrix would correspond to the decreased BET surface area from 599 to 428 m<sup>2</sup>/g. The experimentally found value was 403 m<sup>2</sup>/g (Table 1). Similarly, for 16.7 Ga/M we would expect a BET area of 498 m<sup>2</sup>/g, because of the decreased content of the zeolitic phase in 1 g of sample, and we found 472 m<sup>2</sup>/g. Therefore, we conclude that gallium oxide species do not restrict the access of probe molecules to the internal zeolite pore system, as was observed for ferrierite.<sup>31</sup> The latter zeolite has, however, a much smaller pore system (3.5–5.4 Å).

The amount of  $\beta$ -Ga<sub>2</sub>O<sub>3</sub> in the matrix after various treatments was estimated from XRD diffraction patterns. The sum of peak heights at 30.28°, 33.34°, and 37.26° 2 $\theta$  corresponding to  $\beta$ -Ga<sub>2</sub>O<sub>3</sub> was divided by the sum of peak heights of the zeolite with *hkl* indices of 331, 440, 533, and 642; this was proportional to the ratio  $\beta$ -Ga<sub>2</sub>O<sub>3</sub>/zeolite. In this way ratios of 0.28 and 0.05 were found for the 28.6 Ga/M and 4.8 Ga/M samples, in very good agreement with the amount of  $\beta$ -Ga<sub>2</sub>O<sub>3</sub> initially loaded into the catalysts. For the 28.6 Ga/M sample after calcination in air and reduction with H<sub>2</sub> at 673 K, the ratio decreased to 0.15 and 0.20, respectively (the calculated values were corrected for the loss of crystallinity of the zeolite). According to XRD, considerable amounts of the bulk  $\beta$ -Ga<sub>2</sub>O<sub>3</sub> lost their long-range ordering. Part of the gallium ions was used to fill the vacancies of the matrix. After thermal treatment of 28.6 Ga/M (both in air and hydrogen) the development of minute amounts of an unidentified phase was observed.

We observed the expansion of the lattice parameter of the matrix after the loading of  $\beta$ -Ga<sub>2</sub>O<sub>3</sub>. It is known that incorporation of gallium into the faujasite structure led to the enlargement of the unit cell parameters, due to the longer Ga–O bonds (as compared to Al–O bonds). Such an expansion was observed by Kühl<sup>32</sup> and Szostak.<sup>33</sup> The plot of the lattice parameter *a*<sub>0</sub> of hydrated synthetic Ga–FAU as a function of the number of Ga atoms per unit cell shows two discontinuities, even more pronounced than found for Al–FAU, but the relationship within each region is linear.<sup>32</sup> In the region <64 Ga/uc a linear regression analysis of the data by Kühl gives the expansion of the unit cell as 0.01508 Å/1 Ga. The experimentally observed expansion of *a*<sub>0</sub> for 28.6 Ga/M was in the range 0.157–0.187 Å and corresponded therefore to the insertion of 10.4–12 Ga per unit cell. On the other hand, the expansion of the unit cell of the 4.8 Ga/M sample corresponded to the insertion of only 0.6 Ga/uc. It should be noted, however, that for highly siliceous gallosilicates, similar to aluminosilicates, the plot becomes nonlinear and the estimation of the number of Ga in this region by XRD is inaccurate (the error may be equal to even a few Ga/uc). The lattice of 4.8 Ga/M expanded slightly upon reduction at 873 K, and only traces of the bulk  $\beta$ -Ga<sub>2</sub>O<sub>3</sub> were found in this sample by XRD. This confirmed that most of the gallium oxide in the precursor disappeared upon reduction. The amount of gallium oxide in the precursor corresponded to 6.8 Ga/uc, assuming that all Ga<sub>2</sub>O<sub>3</sub> would be accommodated by the matrix. As XRD has shown only minute amounts of  $\beta$ -Ga<sub>2</sub>O<sub>3</sub> after the reduction, we conclude that about 5 Ga/uc were found in the 4.8 Ga/M catalyst at the tetrahedral sites.

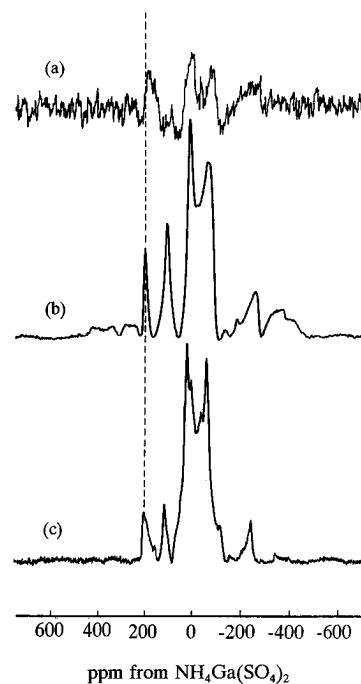


**Figure 3.** <sup>71</sup>Ga MAS NMR spectra of (a) 4.8 Ga/M, (b)  $\beta$ -Ga<sub>2</sub>O<sub>3</sub>, and (c)  $\alpha$ -Ga<sub>2</sub>O<sub>3</sub>.

The unit cell of  $\beta$ -Ga<sub>2</sub>O<sub>3</sub> consists of eight Ga<sup>3+</sup> ions.<sup>34</sup> The gallium ions in this structure adopt tetrahedral and octahedral coordination. Average interionic Ga–O distances are 1.83 Å for tetrahedral and 2.00 Å for octahedral coordination, respectively.<sup>35</sup> Each Ga<sub>I</sub><sup>3+</sup> is surrounded by a distorted tetrahedron of oxygen ions, and each Ga<sub>II</sub><sup>3+</sup> is placed in a highly distorted octahedron of oxygen ions.<sup>35</sup> Those two crystallographically nonequivalent galliums in the unit cell of  $\beta$ -Ga<sub>2</sub>O<sub>3</sub> should give rise to two distinct NMR signals. In Figure 3b the <sup>71</sup>Ga 14 kHz magic-angle-spinning NMR spectrum of  $\beta$ -Ga<sub>2</sub>O<sub>3</sub> taken on a 500 MHz spectrometer is shown. As seen, the spectrum is dominated by spinning sidebands, and contrary to expectation no two distinct gallium signals, corresponding to two different environments of Ga<sup>3+</sup>, can be readily discerned. We note that the central band is not separated from the sidebands. The appearance of the NMR spectrum for  $\alpha$ -Ga<sub>2</sub>O<sub>3</sub>, contaminated with ca. 5% of the  $\beta$  form, is similar, but slight differences are seen upon close inspection (Figure 3c).  $\alpha$ -Ga<sub>2</sub>O<sub>3</sub> is isostructural with  $\alpha$ -corundum, and therefore, all the gallium ions adopt octahedral coordination. As found for  $\beta$ -Ga<sub>2</sub>O<sub>3</sub>, the octahedral coordination gives rise to the signal around 0 ppm, onto which the small, sharp signal of the  $\beta$ -phase around 15 ppm is superimposed. The spinning sidebands for  $\alpha$ -Ga<sub>2</sub>O<sub>3</sub> are also much less intense. There is also a shoulder seen at 105 ppm and assigned to  $\beta$ -phase contamination. This lends support to the assumption that the 105 ppm line in Figure 3b is also a superimposition of a spinning sideband and a real signal coming from tetrahedrally coordinated gallium in  $\beta$ -Ga<sub>2</sub>O<sub>3</sub>. The spectrum of 4.8 Ga/M catalyst, shown in Figure 3a, is different. Despite a lower signal-to-noise ratio, understandable in view of the much lower concentration of gallium species in the catalyst, two features are seen. First, the signal resembling lines of the pure  $\beta$ -Ga<sub>2</sub>O<sub>3</sub> around 0 ppm is seen. Also, the high-intensity spinning sidebands are lost. Second, and most interesting, a line at about 180 ppm, which coincides neither with the spinning sideband at 200 or 105 ppm in pure  $\beta$ -Ga<sub>2</sub>O<sub>3</sub>, with an intensity comparable to that of the line around 0 ppm, is evident. We assign this signal to tetrahedrally coordinated gallium in the zeolitic matrix, in accord with conclusions reached

from IR, Raman, and XRD studies of this sample. NMR studies of gallosilicates, using the  $^{69}\text{Ga}$  and/or  $^{71}\text{Ga}$  resonances, are scarce. Solid-state NMR of gallium nuclei is much more difficult than of  $^{27}\text{Al}$ , because the former gives significantly broader line widths. At the same magnetic field strength, the relative ratio of the line widths for  $^{27}\text{Al}$ ,  $^{69}\text{Ga}$ , and  $^{71}\text{Ga}$  is 1:6.46:2.01.<sup>36</sup> Therefore, of the two gallium nuclei,  $^{71}\text{Ga}$  is the more attractive one. The observed chemical shift of tetrahedral gallium is from 150 to 184, depending on the zeolite structure. For as-prepared gallosilicates with the faujasite structure, containing much more gallium than our sample, the shift was 172 to 174 ppm.<sup>36</sup> The spectrum depicted in Figure 3a constitutes therefore direct evidence that some gallium ions indeed occupy tetrahedral framework sites of the zeolite matrix. Finally, we conclude that strong quadrupolar interactions of the 71 gallium nuclei, observed in our experiments, cannot be effectively removed even using the highest currently available field (500 MHz for protons) and a very fast spinning of the rotor (14 kHz). The quantitative analysis of such spectra is possible only by numerical simulation of the line shape. This work is now in progress.

Raman spectroscopy has been scarcely used for characterization of aluminosilicates, partly due to the high fluorescence encountered when using conventional helium or argon lasers. Fluorescence which masks the weak Raman signals can sometimes be suppressed, e.g., by repeating calcination of a sample before measurement. The introduction of the Nd:YAG laser, with an exciting line at  $\lambda = 1046$  nm, significantly reduced the fluorescence that so hampers conventional excitation sources. The Raman spectrum of the zeolitic matrix is shown in Figure 4c. Contrary to Na-X, Na-Y, and other zeolites, the two strongest bands were observed at 506.5 and 488.8  $\text{cm}^{-1}$  in the acid-extracted US-Y-ex sample. In sodium faujasite the single band at 515 for Na-X and 505  $\text{cm}^{-1}$  for Na-Y has been assigned to the motion of the oxygen atom in the plane perpendicular to the T-O-T bond.<sup>37</sup> There is a shift of 10  $\text{cm}^{-1}$  upon increasing the Si/Al ratio in a faujasite substitutional series (zeolites X and Y). In the case of ultrastable zeolite Y the strongest Raman signal was split into two bands.

The position of a band around 500  $\text{cm}^{-1}$  is a function of the average T-O-T angles for different zeolites.<sup>38</sup> Accordingly, the band at 506.5  $\text{cm}^{-1}$  corresponds to the 142.0° and the band at 488.8  $\text{cm}^{-1}$  to the 146.9° T-O-T angle. In faujasite there are four nonequivalent oxygen atoms, and hence each Si atom has four different Si-O-T angles (T = Si or Al). In natural faujasite<sup>39</sup> these are 138.6°, 139.7°, 145.3°, and 147.4°, while in modified faujasite<sup>40</sup> the four angles are 136.1°, 142.4°, 146.0°, and 149.8°. There are thus two pairs of similar angles, the smaller and the larger angles. The average angle of each pair is 139.2° and 147.1°. The splitting of the band around 500  $\text{cm}^{-1}$  is consistent with the Si-O-T angles of faujasite. Obviously, due to the width of the bands, separate signals for each of the four angles in faujasite were not observed. It follows that Raman spectroscopy is a very sensitive tool and can provide accurate structural information on the subtle changes in the structure of modified faujasite, in addition to X-ray<sup>39</sup> or neutron diffraction studies.<sup>40</sup>

Other much weaker bands were seen at 299, 356, 665, and 815  $\text{cm}^{-1}$ . Upon mixing with gallium(III) oxide both bands of the oxide and those of the matrix were found. The bands related to the bulk gallium oxide were found (Figure 4d) at 347, 416, 653, and 766  $\text{cm}^{-1}$ . After the reduction in hydrogen the appearance of the spectrum changed significantly. The features characteristic of the matrix disappeared. However, the zeolite retained its crystallinity as seen from IR and XRD data. The

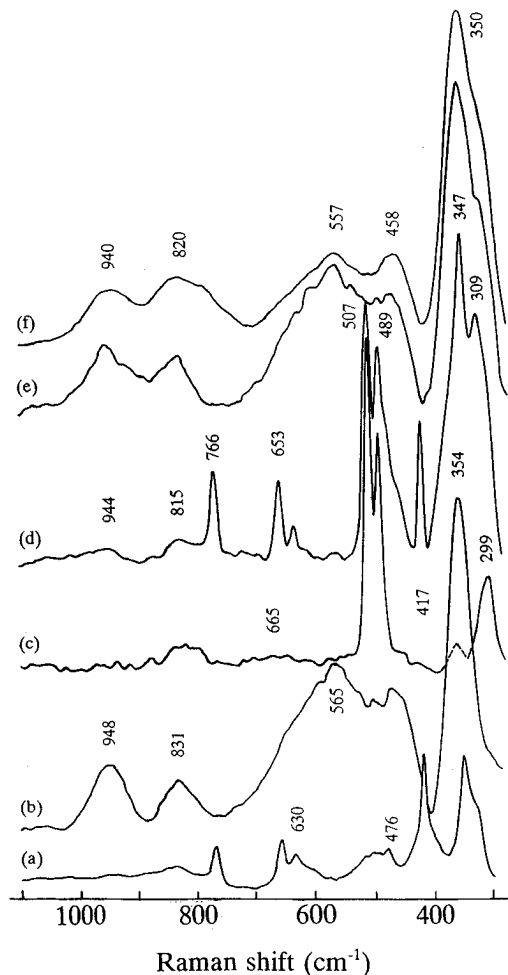


**Figure 4.** FT laser Raman spectra of (a) spectroscopically pure  $\beta\text{-Ga}_2\text{O}_3$ , (b) a stoichiometric mixture of  $\beta\text{-Ga}_2\text{O}_3 + \text{Ga}$  after reduction at 600 °C in a vacuum-sealed ampule, (c) US-Y-ex (M), and 28.6 Ga/M as-prepared (d), and after reduction with hydrogen at 400 °C (e) and 600 °C (f).

lines characteristic of bulk  $\beta\text{-Ga}_2\text{O}_3$  (416, 653, and 766  $\text{cm}^{-1}$ ) also disappeared completely. The signal at ca. 350  $\text{cm}^{-1}$  was broadened. The new broad and weak signals appear in the spectrum upon reduction at 568, 827, and 957  $\text{cm}^{-1}$ . A separate TPR experiment has shown that the bulk  $\beta\text{-Ga}_2\text{O}_3$  was nonreducible by hydrogen at 873 K. However, the same features as found for the reduced 28.6 Ga/M sample were observed for gallium oxide reduced deliberately by pure gallium under vacuum at 873 K.  $\beta\text{-Ga}_2\text{O}_3$  gives lines at 346, 416, 476, 630, 653, and 766  $\text{cm}^{-1}$  (Figure 4a). The bands in the range 300–600  $\text{cm}^{-1}$  correspond to bending vibrations, while the bands above 600  $\text{cm}^{-1}$  are due to the Ga-O<sub>4</sub> tetrahedral stretching modes.<sup>41</sup> The signals of the reduced oxide are seen at 354, 565, 831, and 948  $\text{cm}^{-1}$ . The appearance of the bands is the same as in 28.6 Ga/M reduced with H<sub>2</sub> (cf. Figure 4e,f). Gallium oxide loaded onto ultrastable faujasite was therefore amenable to the reduction by hydrogen, in a way resembling the behavior of the Ga<sub>2</sub>O<sub>3</sub>/ZSM-5 system.<sup>42,43</sup>

The zeolite matrix containing 28.6 wt %  $\beta\text{-Ga}_2\text{O}_3$  gave a typical IR spectrum with the frequencies corresponding both to the matrix and to the oxide. Upon reduction the signal of the bulk  $\beta\text{-Ga}_2\text{O}_3$  at 668  $\text{cm}^{-1}$  decreased, while the main asymmetric stretching vibration of the zeolite at 1072  $\text{cm}^{-1}$  was shifted to 1070 and 1053  $\text{cm}^{-1}$  after the reduction at 400 and 600 °C, respectively. Such a shift to lower wavenumbers is expected upon the formation of the less siliceous framework.<sup>24</sup> The shift of the main stretching frequency might be interpreted

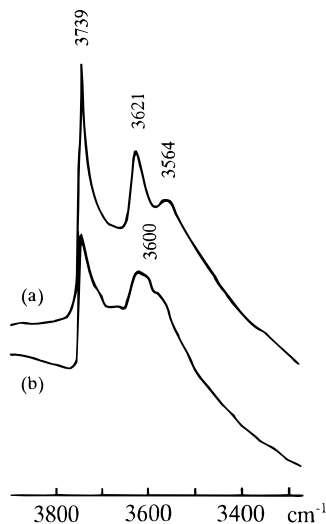


**Figure 5.** FT IR spectra in the hydroxyl vibration region of (a) US-Y-ex (M) and (b) 9.1 Ga/M reduced with hydrogen.

as isomorphous substitution of some gallium into the framework. The ratio of the frequency for  $\beta$ -Ga<sub>2</sub>O<sub>3</sub> at 668 cm<sup>-1</sup> to the matrix frequency at 832 cm<sup>-1</sup> changed from 1.4 to 0.5, which confirmed further the loss of some bulk gallium oxide in the reduced sample and transport of gallium (probably as Ga<sub>2</sub>O<sup>42</sup>) to faujasite cages.

The IR spectrum of the faujasite matrix US-Y-ex (M) after evacuation at 600 °C is shown in Figure 5a. Three well resolved bands are clearly seen, superimposed onto a broader one. The band at 3739 cm<sup>-1</sup> is due to terminal Si-OH group vibrations, while the bands at 3621 and 3564 cm<sup>-1</sup> correspond to high- (HF) and low-frequency (LF) bands of structural Si-O(H)-Al vibrations. The HF band is shifted from its normal position in zeolite Y to lower frequencies, as the Si/Al ratio of the zeolite is increased due to dealumination (Table 1). The broad band with the maximum at 3550 cm<sup>-1</sup> arises from the interaction of silanol groups via hydrogen bonding.<sup>44</sup>

After loading with  $\beta$ -Ga<sub>2</sub>O<sub>3</sub> followed by reduction with hydrogen the IR spectra change significantly. This is exemplified by 9.1 Ga/M (Figure 5b). The bands are now broader; the band of the Si-OH groups is seen at 3742 cm<sup>-1</sup>, while the bands of the structural Si-O(H)-Al groups at 3621 cm<sup>-1</sup> and hydrogen-bonded silanol groups are less intensive. The LF band is seen as a shoulder superimposed on the band of the hydrogen-bonded Si-OH groups. A novel band arises in the spectrum, with the maximum at about 3600–3603 cm<sup>-1</sup>.

Adsorption of ammonia reveals more details in the OH vibration region of the samples. The corresponding difference spectra of M, 4.8 Ga/M, and 9.1 Ga/M, shown in Figure 6, indicate that all the OH groups interact with NH<sub>3</sub>. The band at 3739 cm<sup>-1</sup> in M (Figure 5a) splits into two at 3740 and 3746 cm<sup>-1</sup>, so at least two silanol groups are present in the gallium oxide modified samples (Figure 6b,c). The other bands are present at 3624, 3563, and 3600–3603 cm<sup>-1</sup>. The former two correspond to the same groupings as in the pure matrix (Figure 5a). The band at 3600–3603 cm<sup>-1</sup>, not found in the matrix, is assigned to structural groups of the type Si-O(H)-Ga, which are formed by insertion of some gallium into tetrahedral positions of faujasite. The intensity of this band does not change with the content of gallium oxide in the precursor. This confirms, in accord with NMR studies, that the amount of tetrahedral gallium is essentially the same in 4.8 and 9.1 Ga/M samples (cf. Table 3).

Oxidative dehydrogenation of propane in the presence of oxygen was studied on the spectroscopically pure  $\beta$ -Ga<sub>2</sub>O<sub>3</sub>, the

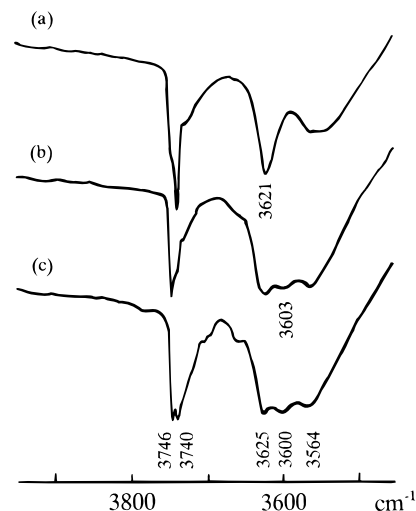


**Figure 6.** FT IR difference spectra in the hydroxyl vibration region after ammonia adsorption at 0.001 T on (a) US-Y-ex (M), (b) 4.8 Ga/M, and (c) 9.1 Ga/M. Samples b and c were reduced *ex situ* with H<sub>2</sub> prior to measurement.

**TABLE 4: Oxidative Dehydrogenation of Propane on  $\beta$ -Ga<sub>2</sub>O<sub>3</sub> and Zeolite Catalysts. Conversion (mol %) and Selectivity (%) to Hydrocarbons**

sample	temp (K)	conversion (%)	selectivity (%) to		
			methane	ethene	propene
$\beta$ -Ga <sub>2</sub> O <sub>3</sub>	773	0.63	5.94	14.15	29.94
	823	2.62	6.38	18.84	33.61
	848	4.82	7.11	20.25	34.39
	873	8.21	8.31	23.50	31.41
US-Y-ex	773	2.96	3.04	8.08	39.01
	798	4.95	1.65	5.74	33.69
	823	7.76	2.01	6.76	28.56
	848	11.84	2.86	8.66	26.29
4.8 Ga/M	773	1.49	5.39	14.10	58.43
	798	3.54	2.94	9.18	43.21
	823	6.74	2.48	7.93	33.22
	848	10.37	3.18	9.36	28.62
28.6 Ga/M	773	2.00	4.97	11.90	48.17
	798	3.77	4.58	11.89	43.54
	823	4.52	3.67	11.19	43.13
	848	8.56	3.95	10.94	30.73

zeolitic matrix, and on the matrix loaded with various amounts of gallium oxide. All the catalysts were reduced in hydrogen before the tests. The homogeneous reaction of propane was studied separately using a microreactor filled with SiC chips while keeping all the other parameters constant. By redesigning the catalytic setup and applying proper test conditions we were able to suppress the homogeneous reaction of propane to 0.3–3% at 773–873 K.

The main products formed from propane on Ga<sub>2</sub>O<sub>3</sub> were propene, ethene, methane, CO, and CO<sub>2</sub>. The total conversion of C<sub>3</sub>H<sub>8</sub> in the presence of oxygen was much lower than those reported for anaerobic conditions.<sup>45</sup>

The results of catalytic tests are shown in Table 4. The conversion level was kept below 10% to observe the primary products of the reaction. The activation energy on all the catalysts was in the range 24.2–34.8 kcal/mol, thus diffusion effects did not affect the results. The conversion of propane on pure gallium oxide is 2 times higher than that corresponding to the homogeneous reaction of propane.

The activity of pure US-Y-ex (M) in the presence of oxygen was relatively high under the conditions used, going from 3% at 773 K to 12% at 848 K. The main products on M were the same as on gallium oxide, but the selectivity to propene was lower. Contrary to ZSM-5, not even traces of aromatic

hydrocarbons were found in the products. The matrix contained the Brønsted acid sites ( $3621\text{ cm}^{-1}$  OH groups); their strength was, however, not high enough to catalyze aromatization of ethene and propene. Consecutive reactions of olefins formed on MFI zeolites lead to the formation of aromatic products. The activation of propane on M is due to Brønsted acid sites, in agreement with other studies.<sup>46,47</sup> We have recalculated catalytic results for M to compare with ZSM-5.<sup>48</sup> The estimated conversion of propane on M under the conditions used with ZSM-5 was 27% as compared to 35% on the latter, thus the activity of faujasite is slightly lower than that of ZSM-5.

The conversion of propane on two catalysts containing gallium is compared in Table 4. It follows that introduction of gallium affects the overall activity; there is, however, not much difference between the two solids (their BET areas are similar, cf. Table 1). The products of propane conversion are the same as on gallium oxide and M. No aromatics were found in the effluents. The most effective catalyst was 4.8 Ga/M, which contained gallium dispersed in the framework of faujasite, and on which traces of the bulk gallium oxide were found after the reduction. Introduction of further amounts of gallium to give the catalyst with a total of 10–12 Ga per unit cell did not lead to increased activity and selectivity of propane conversion. Introduction of gallium into the faujasitic matrix enhanced the selectivity toward propene. The effect was already significant for 4.8 Ga/M, and we conclude that the presence of small amounts of dispersed gallium (ca. 6 Ga/uc) was responsible for the enhanced selectivity to propene.

## Conclusions

Interaction of pure gallium(III) oxide with the US-Y-ex matrix is a complex phenomenon. Pure gallium oxide cannot be reduced by hydrogen at temperatures up to 873 K. However, gallium oxide is easily reduced after contact with the zeolite, which is clearly seen from Raman, XRD, and IR measurements. Reduced gallium oxide is transferred to the channel system of faujasite. Some of the gallium ions are inserted into the zeolite tetrahedral sites (thus healing defects created during the acid treatment of the ultrastable zeolite), while the remaining ones occupy extraframework positions. Further dealumination of the matrix proceeds simultaneously during the high-temperature reduction of the catalyst precursors. As a result about 5–7 Al/uc are expelled into extraframework positions. The remaining aluminum vacancies are filled with silicon coming from amorphous silica. We evidenced it by observing the disappearance of the NMR signal at ca.  $-115$  ppm. When the amount of gallium oxide mixed with the matrix is increased further, the situation does not change significantly. More aluminum is depleted in the framework, but the amount of tetrahedral gallium remains essentially the same. The maximum amounts of tetrahedral gallium which can still be accommodated by the matrix is low and does not exceed about 6 Ga per unit cell. Framework gallium gives rise to structural hydroxyl groups Si–O(H)–Ga, seen in the IR spectra at  $3600\text{--}3603\text{ cm}^{-1}$ . Such groups are not present in the pure zeolitic matrix.

All the samples show activity in the oxidative dehydrogenation of propane. The highest conversion level of propane was observed for pure US-Y-ex zeolite. The matrix itself is very active in the conversion of propane. Contrary to the H-ZSM-5/Ga<sub>2</sub>O<sub>3</sub> system no aromatics were found in the reaction products under the conditions studied. Loading of the ultrastable zeolite with increasing amounts of  $\beta$ -Ga<sub>2</sub>O<sub>3</sub> gives rise to the continuous decrease of the overall conversion level of propane, while the enhanced selectivity to propene is still observed. It is interesting that the already few gallium ions accommodated by

the matrix significantly increase the selectivity to propene. This is due to the decreasing amount of strong acid centers Si–O(H)–Al and forming simultaneously new hydroxyl groups Si–O(H)–Ga. As further loading with active phase does not change the reaction selectivity, we can conclude that the first gallium ions introduced into the framework form the active centers for transformation of propane. The gallium-containing catalysts based on the ultrastable zeolite Y constitute therefore an interesting system for a selective transformation of low molecular weight alkanes to olefins.

**Note Added in Proof.** After submitting the manuscript, we found a recent <sup>69</sup>Ga and <sup>71</sup>Ga NMR study of  $\beta$ -Ga<sub>2</sub>O<sub>3</sub> by Massiot et al. [Massiot, D.; Farnan, I.; Gautier, N.; Trumeau, D.; Trokiner, A.; Coutures, J. P. *Solid State Nucl. Magn. Reson.* **1995**, *4*, 241]. The octahedral and tetrahedral sites of gallium ions in this oxide have been fully characterized. That work provides a further support for the interpretation of our results.

**Acknowledgment.** We are grateful to the State Committee for Scientific Research, Warsaw, for support (Grant No. 2 P303 149 04). Thanks are also due to Dr. S. Steuernagel of Bruker (Karlsruhe, Germany) for <sup>71</sup>Ga MAS NMR spectra. The excellent technical assistance of Ms. J. Kryściak is also acknowledged.

## References and Notes

- (1) Mowry, J. R.; Anderson, R. F.; Johnson, J. A. *Oil Gas J.* **1985**, *83*, 128.
- (2) Mowry, J. R.; Martindale, D. C.; Hall, H. P. *Arab. J. Sci. Eng.* **1985**, *10*, 367.
- (3) Sulikowski, B.; Klinowski, J. *J. Chem. Soc., Chem. Commun.* **1989**, 1289 and references therein.
- (4) Thomas, J. M.; Xinsheng, L. *J. Phys. Chem.* **1986**, *90*, 4843.
- (5) Liu, X.; Lin, J.; Liu, X.; Thomas, J. M. *Zeolites* **1992**, *12*, 936.
- (6) Kanazirev, V.; Price, G. L.; Dooley, K. M. *J. Chem. Soc., Chem. Commun.* **1990**, 712.
- (7) Kanazirev, V.; Dimitrova, R.; Price, G. L.; Khodakov, A. Yu.; Kustov, L. M.; Kazansky, V. B. *J. Mol. Catal.* **1991**, *70*, 111.
- (8) Carli, R.; Bianchi, C. L.; Giannantonio, R.; Ragaini, V. *J. Mol. Catal.* **1993**, *83*, 379.
- (9) Zulfugarov, Z. G.; Suleimanov, A. S.; Samedov, Ch. R. In *Structure and Reactivity of Modified Zeolites*; Jacobs, P. A., Jaeger, N. I., Jiru, P., Kazansky, V. B., Schulz-Ekloff, G., Eds.; Elsevier: Amsterdam, 1984; *Stud. Surf. Sci. Catal.* **1984**, *18*, 167.
- (10) Ione, K. G.; Vostrikova, L. A.; Petrova, A. V.; Mastikhin, V. M. Ref 9, p 151.
- (11) McDaniel, C. V.; Maher, P. K. In *Molecular Sieves*; Society of Chemical Industry: London, 1968; p 186.
- (12) Kerr, G. T.; Shipman, G. F. *J. Phys. Chem.* **1968**, *72*, 3071.
- (13) Kerr, G. T.; Chester, A. W.; Olson, D. H. In *Proceedings of the Symposium on Zeolites*, 11–14 September, 1978, Szeged, Hungary, *Acta Phys. Chem. Szeged, Nova Ser.* **1978**, *24*, 169.
- (14) Scherzer, J. J. *Catal.* **1978**, *54*, 285.
- (15) Sulikowski, B.; Rakoczy, J.; Hamdan, H.; Klinowski, J. *J. Chem. Soc., Chem. Commun.* **1987**, 1542.
- (16) Man, P. P.; Klinowski, J. *J. Chem. Soc., Chem. Commun.* **1988**, 1291.
- (17) Man, P. P.; Klinowski, J.; Trokiner, A.; Zanni, H.; Papon, P. *Chem. Phys. Lett.* **1988**, *151*, 143.
- (18) Maesen, T. L. M.; Sulikowski, B.; van Bekkum, H.; Kouwenhoven, H. W.; Klinowski, J. *Appl. Catal.* **1989**, *48*, 373.
- (19) Engelhardt, G.; Lohse, U.; Lippmaa, E.; Tarmak, M.; Mägi, M. Z. *Anorg. Allg. Chem.* **1981**, *482*, 49.
- (20) Klinowski, J.; Ramdas, S.; Thomas, J. M.; Fyfe, C. A.; Hartman, J. S. *J. Chem. Soc., Faraday Trans. 2* **1982**, *78*, 1025.
- (21) Barer, R. M.; Makki, M. B. *Can. J. Chem.* **1964**, *42*, 1481.
- (22) Lee, F. T.; Rees, L. V. C. *J. Chem. Soc., Faraday Trans. 1* **1987**, *83*, 1531.
- (23) Sohn, J. R.; DeCanio, S. J.; Lunsford, J. H.; O'Donnell, D. J. *Zeolites* **1986**, *6*, 225.
- (24) Sulikowski, B.; Klinowski, J. *J. Chem. Soc., Faraday Trans.* **1990**, *86*, 199.
- (25) Fichtner-Schmittler, H.; Lohse, U.; Engelhardt, G.; Patzelová, V. *Cryst. Res. Technol.* **1984**, *19*, K1.
- (26) Sulikowski, B. *Heterogeneous Chem. Rev.* **1996**, *3* (3), 171.

- (27) Freude, D.; Fröhlich, T.; Hunger, M.; Pfeifer, H.; Scheler, G. *Chem. Phys. Lett.* **1983**, *98*, 263.
- (28) Klinowski, J.; Thomas, J. M.; Fyfe, C. A.; Gobbi, G. C.; Hartman, J. S. *Inorg. Chem.* **1983**, *22*, 63.
- (29) Ray, G. J.; Nerheim, A. G.; Donohue, J. A. *Zeolites* **1988**, *8*, 458.
- (30) Engelhardt, G.; Michel, D. *High-Resolution Solid-State NMR of Silicates and Zeolites*; Wiley: Chichester, New York, 1987; p 254.
- (31) Cortés Corberán, V.; Valenzuela, R. X.; Sulikowski, B.; Derewiński, M.; Olejniczak, Z.; Kryściak, J. Fifth European Workshop Meeting on Selective Oxidation by Heterogeneous Catalysis, Berlin, 1995.
- (32) Kühl, G. H. *J. Inorg. Nucl. Chem.* **1971**, *33*, 3261.
- (33) Szostak, R. *Molecular Sieves*; Van Nostrand Reinhold: New York, 1989; p 214.
- (34) Kohn, J. A.; Katz, G.; Broder, J. D. *Am. Mineral.* **1957**, *42*, 398.
- (35) Geller, S. *J. Chem. Phys.* **1960**, *33*, 676.
- (36) Timken, H. K. C.; Oldfield, E. *J. Am. Chem. Soc.* **1987**, *109*, 7669.
- (37) Dutta, P. K.; Shieh, D. C. *J. Phys. Chem.* **1986**, *90*, 2331.
- (38) Dutta, P. K.; Shieh, D. C.; Puri, M. *Zeolites* **1988**, *8*, 306.
- (39) Olson, D. H.; Dempsey, E. *J. Catal.* **1969**, *13*, 221.
- (40) Barrie, P. J.; Gladden, L. F.; Klinowski, J. *J. Chem. Soc., Chem. Commun.* **1991**, 592.
- (41) Dohy, D.; Lucazeau, G.; Revcolevschi, A. *J. Solid State Chem.* **1982**, *45*, 180.
- (42) Le Van Mao, R.; Carli, R.; Yao, J.; Ragaini, V. *Catal. Lett.* **1992**, *16*, 43.
- (43) Price, G. L.; Kanazirev, V. *J. Catal.* **1990**, *126*, 267.
- (44) de Ruiter, R.; Kentgens, A. P. M.; Grootendorst, J.; Jansen, J. C.; van Bekkum, H. *Zeolites* **1993**, *13*, 128.
- (45) Meriaudeau, P.; Naccache, C. *J. Mol. Catal.* **1990**, *59*, L31.
- (46) Buckles, G.; Hutchings, G. J.; Williams, C. D. *Catal. Lett.* **1991**, *8*, 115.
- (47) Derouane, E. G.; Abdul Hamid, S. B.; Ivanova, I. I.; Blom, N.; Højlund-Nielsen, P.-E. *J. Mol. Catal.* **1994**, *86*, 371.
- (48) Paredes Quesada, N. Ph.D. Thesis, Universidad Autónoma, Madrid, 1993.

JP9604507